Progress In Electromagnetics Research C, Vol. 73, 9–16, 2017

Broadband Perfect Metamaterial Absorber on Thin Substrate for X-Band and Ku-Band Applications

Gobinda Sen[1, *], Sk. Nurul Islam[1], Amartya Banerjee[2], and Santanu Das[1]

Abstract—A broadband Perfect Metamaterial Absorber (PMA) on FR-4 Epoxy substrate for X-band and Ku-Band applications is proposed. The unit cell structure is composed of rectangular patches of appropriate shapes and orientation on top of the metal-backed dielectric substrate having a thickness of 2.7 mm ($0.16\lambda_L$). The relative absorption bandwidth is 79% (more than 85% absorption) covering the entire X-band and the Ku-Band of the microwave frequencies. The surface current distributions of the top and bottom planes have been analyzed to elaborate the absorption mechanism of the structure. The broadband characteristics of the design support its claim of being useful to a wide range of applications in both commercial and research sectors. Such applications include military and stealth devices, thermal sensors and electronic-cloaking devices.

1. INTRODUCTION

Perfect Metamaterial Absorbers (PMA) utilizing periodic/non-periodic random structures on dielectrics have gathered adequate research interest over the past years owing to their exquisite properties and performances, along with their simple fabrication techniques [1]. Composed of artificial unit-cell structures, metamaterials have gained popularity in microwave research due to their exotic properties showcased and utilized in the negative refraction phenomena [2], sub-wavelength imaging, super-lens [3], sensor applications [4–6], millimeter wave applications [7] and invisible cloaking materials [8] unveiling a sector of boundless opportunities. From solar cell applications [9] to energy harvesting from microwaves [10], metamaterial absorbers have nowadays become one of the most relevant areas of research interests. Previously, while developing broadband absorbers, Jaumann Screens and lossy Frequency Selective Surfaces (FSS) were the preferred candidates for the purpose [11]. However, the thickness of such absorbers being more, made them bulky and not-so-preferred for applications, as absorbers on thinner substrate materials started to develop gradually with time.

With the advent of metamaterial absorbers, people got the interest to improve the Salisbury Screen and Jaumann Screen type absorbers by trying to replace the continuous resistive patterns with periodic arrays of resistive patches on thin metallic-ground-backed substrates [12]. Also, for broadband application numerous other structures were proposed using Hilbert Curves, reactive impedance ground planes, or lumped element loaded structures [13], however they all suffer from high substrate thickness ($\sim \lambda/4$) with respect to their lowest operating frequencies.

In the literature [14, 16], the authors proposed multilayered absorbers with relative absorption bandwidths of 53.10% (with an absorber thickness = $0.23\lambda L$) and 93.51% (with an absorber thickness = $0.17\lambda L$) respectively. However due to the complex multilayered unit-cell structures, the design complexity increases. In [15] a higher absorption bandwidth is reported but the thickness has increased. The previous work [16] of the authors of this paper proposed a single layer absorber with a

Received 11 January 2017, Accepted 27 March 2017, Scheduled 4 April 2017

* Corresponding author: Gobinda Sen (gobinda.dets@gmail.com).

[1] Department of Electronics and Telecomm. Engineering, Indian Institute of Engineering Science and Technology, Shibpur, Howrah, India. [2] Department of Electronics and Tele-Communication Engineering, Jadavpur University, Jadavpur, Kolkata, India.

substrate thickness of 2.7 mm ($0.12\lambda L$) with a simple unit cell structure for X band applications. In this paper, the proposed work tries to generate a higher absorption bandwidth with the same dimensions so as to cater to both X and Ku band applications. In this article, a broadband absorber on an FR-4 Epoxy substrate, having a thickness of 2.7 mm only ($\sim 0.16\lambda_L$) is proposed, which qualifies for a compact absorber having a sufficiently high absorption bandwidth ranging from 7.77 GHz to 17.98 GHz, which is suitable for both X-Band and Ku-Band applications. The design procedures of the structure are explained in Section 2, the results are analyzed in Section 3 and the paper is concluded in Section 4 with a brief overview of the features of the proposed work.

2. ABSORBER DESIGN

The unit cell of the absorber is shown in Fig. 1 with the dimensions listed in Table 1. The design started with two L-shaped patches facing each other with the longer sides coupled in a broadside manner. The structure returned a broadband absorption performance from 9 GHz to 16.8 GHz, having an absorptivity greater than 0.8 or 80% over the frequency range as shown in Fig. 3(a) (black dotted line). To improve the coupling between the patches a rectangular conductor strip is inserted between them, as the bandwidth widened from 7.9 GHz to 17.9 GHz as shown in Fig. 3(a) (red dash dotted line). To further improve the absorptivity and obtain a still higher bandwidth horizontal metallic strips of length 'p' and width 'w' are added over the horizontal arms of the L-shaped patches, hence to improve the capacitive coupling between two adjacent unit cells. This resulted in a further increase in the absorption bandwidth ranging from 7.92 GHz to 18.12 GHz, covering both the X-band and the Ku-band of operations as shown in Fig. 3(a) (blue solid line). The unit cell is developed on a substrate slab having dimensions 9 mm × 9 mm in length and breadth respectively. The dimensions are given below in Table 1.

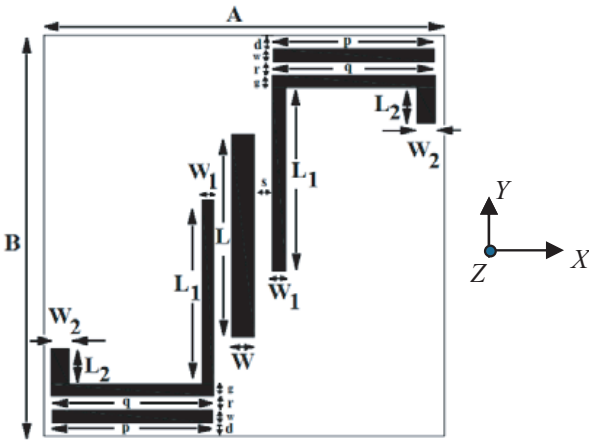

Figure 1. Unit cell of the PMA structure.

Table 1. Designed dimensions of the proposed structure.

A	B	L	W	L_1	W_1	L_2	W_2	p	q	s	g	r	w	d
9	9	4.55	0.5	4.4	0.3	0.8	0.4	3.6	3.5	0.4	0.27	0.25	0.3	0.3

3. ANALYSIS OF THE PMA

The absorption phenomena of the PMA can be better understood with the transmission line modeling [18] of the whole structure as shown in Fig. 2.

The equivalent circuit model of the metallic patches is composed of a resistor (R), a capacitor (C) and an inductor (L) connected in series. The etched gap area between two strips as in Fig. 1 formed

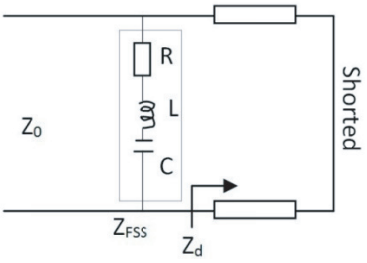

Figure 2. Transmission line model of the PMA.

the series capacitor. The impedance of the periodic structure is written as:

$$Z_{FSS} = R + j\omega L + 1/j\omega C = R - j\left(\frac{1-\omega^2 LC}{\omega C}\right) \tag{1}$$

The periodic unit cell layout influences the values of L, C and R parameters. The impedance of the dielectric substrate with the metal back plane is represented as:

$$Z_d = jZ_c^{TE,TM}\tan(\beta d) \tag{2}$$

where $Z_c^{TE} = (\omega\mu_o\mu_r)/\beta$ and $Zc^{TM} = \beta/(\omega\epsilon_o\epsilon_r)$ are the characteristic impedance of the dielectric substrate with metal plate. $\beta = (\omega/C_0) * \sqrt{\varepsilon_r\mu_r - \sin^2\theta}$ is the propagation constant along the normal of the dielectric substrate with θ denoting the incident angle of the incident wave with respect to the normal. C_0 is the wave velocity in the vacuum. The surface impedance Z_s of PMA is equal to the parallel connection between the impedance Z_{FSS} of the periodic structure and the impedance Z_d of the dielectric substrate with the metal plate. After some manipulation the real part of input impedance Z_s as seen from the air can be derived:

$$\mathrm{Re}\{Z_s\} = \frac{RZ_d^2}{[(1-\omega^2 LC)/\omega C - Z_d]^2 + R^2} \tag{3}$$

In order to obtain absorption of the incoming signal, the impedance $\mathrm{Re}\{Z_s\}$ should match to the free space impedance Z_0:

$$R_{opt} = \frac{(Z_c^{TE,TM})^2\tan^2(\beta d)}{Z_0^{TE,TM}} \tag{4}$$

where $Z_0 = \sqrt{(\mu_0/\epsilon_o)}/\cos\theta$ for TE waves, $Z_0 = \sqrt{(\mu_0/\epsilon_o)}/\cos\theta$ for TM waves. The relation (4) highlights the dependence of the optimal FSS resistance on the thickness and the permittivity of the substrate.

One can recall the fundamental working formula (5) for such a design that relates Absorption with Reflection and Transmission Coefficients of the structure, viz.

$$A(\omega) = 1 - R(\omega) \tag{5}$$

where, $R(\omega)$ is the reflection coefficient as a function of frequency. So, in order to maximize absorption, one needs to minimize the reflection as can be seen from the equation above or the real part of the effective normalized impedance should be near to unity.

4. SIMULATED AND EXPERIMENTAL RESULTS

The simulated absorptivity performances of the proposed structure are observed for both the TE and TM polarizations of the incident waves as given in Figs. 3(a) and (b), respectively. The Fig. 3(a) includes the absorptivity plot obtained from the initial structure with two L-shaped patches facing each other, the plot with the improved performance when a coupling strip is inserted in between the patches, and the final plot corresponding to the proposed structure. The result shows an overall good absorption for both the polarizations of incident waves and hence makes the structure polarization insensitive.

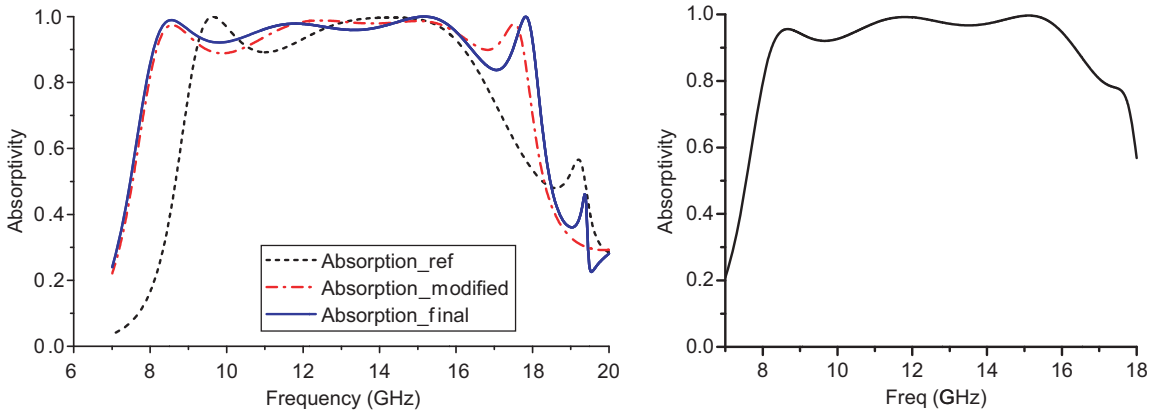

Figure 3. (a) Simulated absorptivity performance of the PMA at different stages with TE Polarization. (b) Optimized design performance at TM polarization.

The normalized effective impedance of the proposed PMA as obtained using effective parameter extraction procedure [19] is shown in Fig. 4 below. Real part of the Impedance is very near to unity, which leads to a broadband absorption over the X band and Ku band of the microwave spectrum.

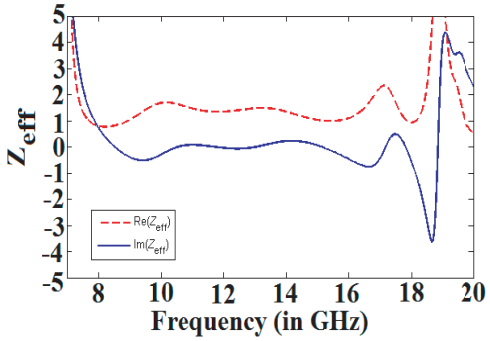

Figure 4. Effective normalized impedance v/s frequency of the PMA.

The simulated absorption performance for different angles (θ) of the incident wave is also studied as shown in Fig. 5. From the results it can be inferred that for both TE and TM polarization, the absorber has a stable performance over the absorption band.

The parametric studies given in Fig. 6 represent the effect of coupling on the absorptivity performance of the PMA as the strip length L changes and an optimum value of the same is found as 4.55 mm. The broadband absorption response is obtained due to the matching of the input impedance $Z(\omega)$ of the structure with the free space impedance $Z_0(\omega)$ over the entire band. From Fig. 6 it can be inferred that initially with an increment in the strip length 'L' the coupling increased and the value of $Z(\omega)$ came closer to the free space impedance. As a result, the absorption performance was optimized at a value of $L = 4.55$ mm, but beyond that length, the performance deteriorated due to a mismatch with the free space impedance.

The surface current distributions at the absorption peaks of 8 GHz and 15 GHz which lies within the absorption bandwidth of the absorber are shown in Figs. 7 and 8, respectively.

The figure shows that the surface currents at 8 GHz on the L-shaped patches and on the coupled strip in the middle are creating a parallel vector, hence determining the effective permittivity value of the component. On the other hand, in between the ground plane and the patch layer, the anti-parallel distribution of the current forms a magnetic loop and hence determines the effective permeability response at that frequency.

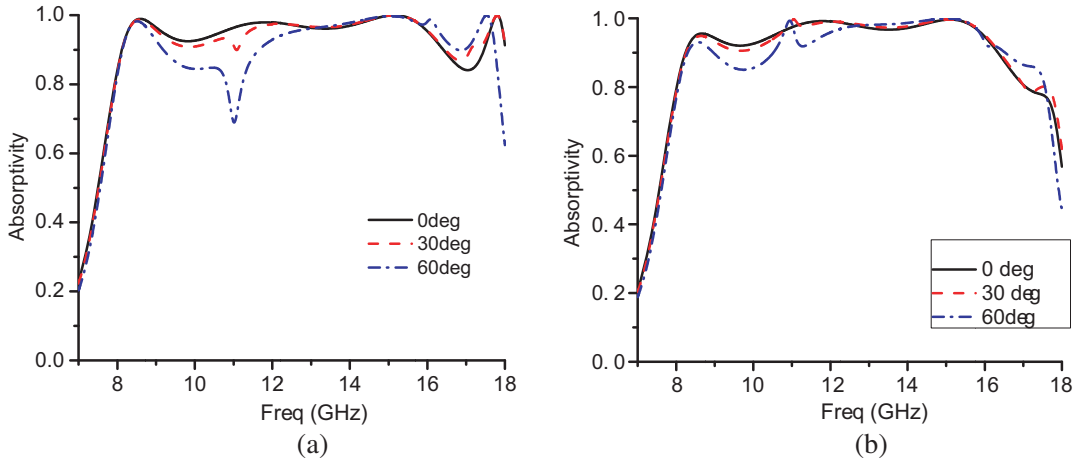

Figure 5. Simulated absorptivity performance of the PMA at different angles of incidence (θ) with (a) TE Polarization, (b) TM polarization.

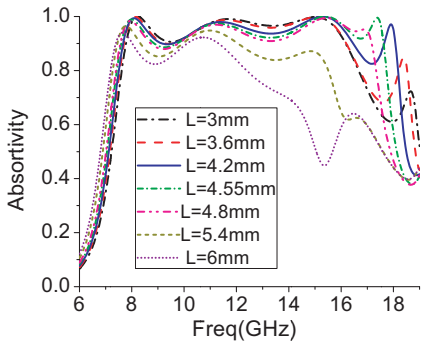

Figure 6. Parametric studies on the absorptivity performance with different values of the vertical strip length (L).

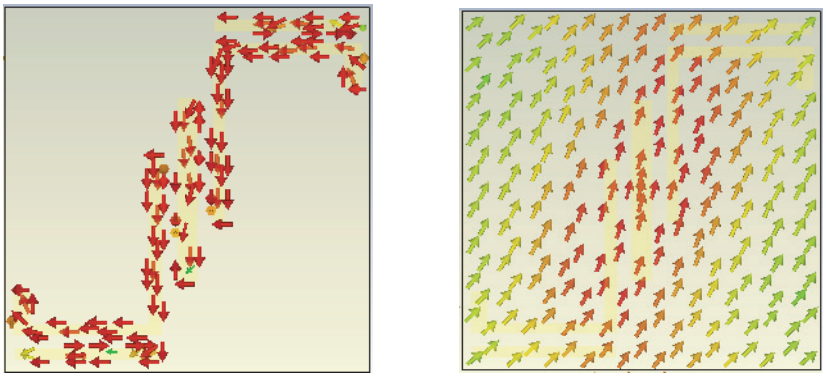

Figure 7. Surface current distributions at 8 GHz on (a) top plane, (b) bottom plane.

However at 15 GHz, as in Fig. 8, surface currents at the L-shaped patches and the coupled strip in the middle are creating an anti-parallel vector, hence giving the effective permeability value of the component, and the parallel current distribution at the two L-shaped strips determines the effective permittivity value. The combined effect gives a metamaterial-like behavior leading to a broadband absorption performance.

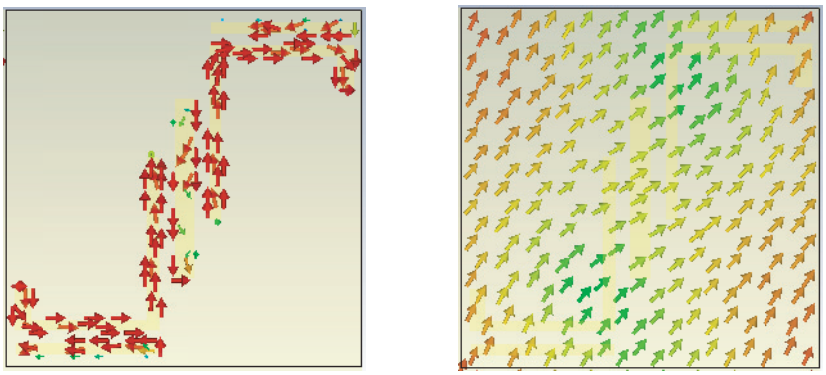

(a) (b)

Figure 8. Surface current distributions at 15 GHz on (a) top plane, (b) bottom plane.

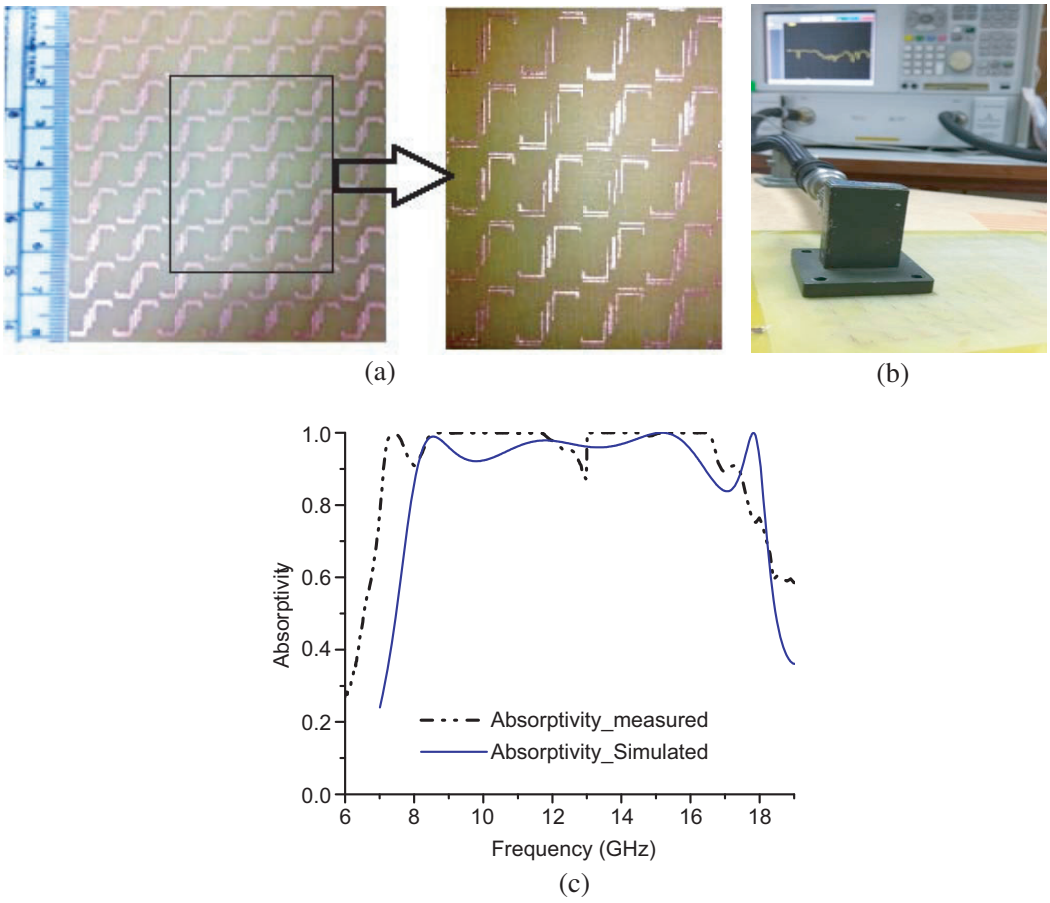

(a) (b) (c)

Figure 9. (a) Fabricated prototype of the absorber. (b) Measurement Setup. (c) Experimental and simulation results.

Experimental results obtained by the waveguide measurement method [20] and the fabricated prototype (81 mm × 63 mm) are shown in Fig. 9(a). Two standard waveguides operating in the X-band and Ku-band and an Agilent N5230A series Network Analyzer are used for the measurement process as in Fig. 9(b).

The number of unit cells used for the measurement is dependent upon the aperture of the waveguides. Here the X-band waveguide is covering more no of unit cells as compared to the Ku-

band guide due to the larger aperture size of the former. The measurement is done with two sets of components, one having the X-band waveguide for the X-band absorption measurement and the other one with Ku-band waveguide for the upper band measurement. There is a little deviation in the simulated and the measurement results as shown in Fig. 9(c) but the absorption band is seen to be covering the entire X and Ku band of microwave spectrum with more than of 80% absorption.

The compared results of the proposed single-layer broadband PMA with other pre-existing wideband absorbers reported in the literatures are given in Table 2, which shows that the proposed PMA excels the other absorbers [14–17] with its compact design and cost-efficient single-layer structure.

Table 2. Comparative studies.

Ref.	Design characteristics	Thickness	Relative Absorption Bandwidth
[14]	Multilayered quadrangular frustum pyramid unit cell.	$0.23\lambda_L$	53.10%
[15]	Unidirectional stand-up resistive film patch unit cell.	$0.96\lambda_L$	148.2%
[16]	Multilayered double split-serration-rings (DSSRs) unit cell.	$0.17\lambda_L$	93.51%
[17]	Single layer unit cell.	$0.12\lambda_L$	60.40%
[proposed]	Single layer low profile unit cell.	$0.16\lambda_L$	79%

5. CONCLUSION

A broadband perfect metamaterial absorber is proposed in this article, for X and Ku band applications, on an FR-4 Epoxy substrate. The absorption bandwidth covers the entire X and Ku bands of operation with more than 85% absorption over the range. The response shows three absorption peaks at 8.48 GHz, 15.4 GHz, and 17.81 GHz respectively having more than 95% absorption at those frequencies. The substrate thickness is only 2.7 mm ($0.16\lambda_L$), which adds to the features of this design, making it a low-profile and less-bulky component that can be widely used for appropriate microwave applications.

REFERENCES

1. Landy, N. I., S. Sajuyigbe, J. J. Mock, D. R. Smith, and W. J. Padilla, "Perfect metamaterial absorber," *Phys. Rev. Lett.*, Vol. 100, 207402, May 2008.
2. Shelby, R. A., D. R. Smith, and S. Schultz, "Experimental verification of a negative index of refraction," *Science*, Vol. 292, No. 5514, April 2001.
3. Pendry, J. B., "Negative refraction makes a perfect lens," *Phys. Rev. Lett.*, Vol. 85, No. 18, October 2000.
4. Bakir, M., et al., "Tunable perfect metamaterial absorber and sensor applications," *Journal of Materials Science: Materials in Electronics*, Vol. 27, 12091–12099, 2016.
5. Dincer, F., et al., "Multi-band polarization independent cylindrical metamaterial absorber and sensor application," *Modern Physics Letters B*, Vol. 30, 1650095-9, 2016.
6. Huang, L. and H. Chen, "Multi-band and polarization insensitive metamaterial absorber," *Progress In Electromagnetics Research*, Vol. 113, 103–110, 2011.
7. Singh, P., S. Kabiri Ameri, L. Chao, M. N. Afsar, and S. Sonkusale, "Broadband millimeterwave metamaterial absorber based on embedding of dual resonators," *Progress In Electromagnetics Research*, Vol. 142, 625–638, 2013.

8. Pendry, J. B., D. Schurig, and D. R. Smith, "Controlling electromagnetic fields," *Science*, Vol. 312, No. 5781, June 2006.
9. Unal, E., et al., "Tunable perfect metamaterial absorber design using the golden radio and energy harvesting and sensor applications," *Journal of Materials Science: Materials in Electronics*, 10.1007/s 10854-015-3642-7.
10. Dincer, F., O. Akgol, M. Karaaslan, E. Unal, and C. Sabah, "Polarization angle independent perfect metamaterial absorbers for solar cell applications in the microwave, infrared, and visible regime," *Progress In Electromagnetics Research*, Vol. 144, 93–101, 2014.
11. Chambers, B. and A. Tennant, "Optimized design of Jaumann radar absorbing materials using a genetic algorithm," *IEE Proc. Radar Sonar and Navig.*, Vol. 143, No. 1, February 1996.
12. Costa, F., A. Monorchio, and G. Manara, "Analysis and design of ultrathin electromagnetic absorbers comprising resistively loaded high impedance surfaces," *IEEE Transactions on Antennas and Propagation*, Vol. 58, No. 5, May 2010.
13. Noor, A. and Z. Hu, "Metamaterial dual-polarized resistive Hilbert curve array radar absorber," *IET Microw. Antennas Propag.*, Vol. 4, No. 6, 667–673, 2010.
14. Ding, F., Y. Cui, X. Ge, Y. Jin, and S. He, "Ultra-broadband microwave metamaterial absorber," *Applied Physics Letters*, Vol. 100, 103506, 2012.
15. Shen, Y., Z. Pei, Y. Pang, J. Wang, A. Zhang, and S. Qu, "An extremely wideband and lightweight metamaterial absorber," *Journal of Applied Physics*, Vol. 117, 224503, 2015.
16. Li, S.-J., X.-Y. Cao, J. Gao, T. Liu, Y.-J. Zheng, and Z. Zhang, "Analysis and design of three-layer perfect metamaterial-inspired absorber based on double split-serration-rings structure," *IEEE Transactions on Antennas and Propagation*, Vol. 63, No. 11, November 2015.
17. Sen, G., A. Banerjee, Sk. Nurul Islam, and S. Das, "Ultra-thin miniaturized metamaterial perfect absorber for X-band application," *Microwave and Optical Technology Letters*, Vol. 58, No. 10, 2367–2370, October 2016.
18. Qiu, K. and S. Feng, "A novel metamaterial absorber with perfect wave absorption obtained by layout design," *Journal of Electromagnetic Waves and Applications*, Vol. 30, No. 4, 523–535, 2016.
19. Szabo, Z., G. H. Park, R. Hedge, and E. P. Li, "A unique extraction of metamaterial parameters based on Kramers-Kronig relationship," *IEEE Transactions on Microwave Theory and Techniques*, Vol. 58, No. 10, 2646–2653, October 2010.
20. Bayatpur, F. and K. Sarabandi, "Tuning performance of metamaterial-based frequency selective surfaces," *IEEE Transactions on Antennas and Propagation*, Vol. 57, No. 2, February 2009.